# Effect of Short-Range Interactions on Polyelectrolyte Adsorption at Charged Surfaces†

**Andrey V. Dobrynin***

*Polymer Program, Institute of Materials Science and Department of Physics, University of Connecticut, Storrs, Connecticut 06269-3136*

**Michael Rubinstein**

*Department of Chemistry, University of North Carolina, Chapel Hill, North Carolina 27599-3290*

*Received: December 5, 2002*

We have studied the effect of short-range interactions on polyelectrolyte adsorption at oppositely and similarly charged surfaces. The properties of the adsorbed layer, such as polymer surface coverage, layer thickness, and surface overcharging (for adsorption at oppositely charged surfaces), are calculated as a function of the surface charge density, the strength of the short-range interactions, and the ionic strength of the solution. The properties of dilute and semidilute two-dimensional adsorbed layers are calculated in the framework of the strongly correlated Wigner liquid model. In these regimes, the surface overcharging by adsorbed polyelectrolyte chains increases as a function of the square root of the salt concentration. At higher surface charge densities, when adsorbed polyelectrolytes form a three-dimensional adsorbed layer, we use the self-consistent mean-field theory to calculate the layer properties. Here, the polymer surface coverage shows nonmonotonic dependence on the salt concentration; it initially increases as the salt concentration increases at low ionic strengths and then decreases as the ionic strength becomes higher than some critical value. The decrease of the surface coverage at a higher salt concentration is due to additional screening of the surface charge by salt ions. We show that the adsorption of polyelectrolytes at similarly charged surfaces can only occur within the range of surface charge densities where the short-range interactions dominate the electrostatic repulsion between adsorbed chains and the charged surface. In these regimes, the salt dependence of the polymer surface coverage and layer thickness is similar to that for polyelectrolyte adsorption at oppositely charged surfaces that are dominated by short-range interactions.

## 1. Introduction

The adsorption of charged polymers at surfaces and interfaces[1−4] is a rapidly growing field of tremendous importance for colloidal science, biophysics, nanoelectronics, etc. Indeed, many practical systems for industrial applications utilize the adsorption properties of charged polymers as stabilizing agents, emulsifiers, rheology modifiers, and agents for nanofabrication that exploit the ability of charged polymers to modify surface properties. All these applications rely on attaching or immobilizing the charged chains at solid surfaces or at liquid/liquid and liquid/air interfaces. This immobilization can occur because of either pure electrostatic interactions or short-range attractive interactions.

This paper continues a series of papers[5−8] that involve the adsorption of charged polymers by extending our model of polyelectrolyte adsorption to the case of the adsorption of charged polymers due to short-range attraction to oppositely, neutral, and similarly charged surfaces. The factors that oppose polymer adsorption can be electrostatic repulsion between adsorbed chains, repulsion from the image chains (if the adsorption occurs at the interface between media with dissimilar dielectric properties, say, at a water/air interface), or electrostatic repulsion from the similarly charged substrate. As in our previous publications,[5−8] we utilize a strongly correlated Wigner liquid approach[9−13] to account for repulsive interactions between adsorbed chains in two-dimensional dilute and semidilute adsorbed layers. In the framework of this approach, the system is divided into Wigner−Seitz cells that surround each polyelectrolyte chain in a dilute adsorbed layer or in a section of polyelectrolyte chain in a semidilute two-dimensional adsorbed layer. In the case of dense adsorbed layers, we apply a mean-field approach that is based on the solution of coupled differential equations describing the distribution of polymer density and electrostatic potential within adsorbed layers.[14−17]

The remainder of the paper is organized as follows. In the next section, we briefly discuss the adsorption of a polyelectrolyte chain at a neutral surface and elucidate the relative importance of different factors that affect chain adsorption. Section 3 is devoted to the adsorption of polyelectrolyte chains because of short-range and electrostatic interactions. We calculate the dependence of surface coverage, surface overcharging, and layer thickness as a function of the salt concentration and the degree of ionization of a polyelectrolyte chain. In section 4, we will generalize the model of polyelectrolyte adsorption described in section 3 to the case of adsorption at similarly charged surfaces.

## 2. Adsorption of a Polyelectrolyte Chain at a Neutral Surface

Consider a flexible polyelectrolyte chain with a degree of polymerization $N$, a fraction of charged monomers $f$, and a bond

† Part of the special issue "International Symposium on Polyelectrolytes".

* Author to whom correspondence should be addressed. E-mail: avd@ims.uconn.edu.

10.1021/jp0225323 CCC: $25.00 
Published on Web 07/11/2003

length $a$ in a solvent with Bjerrum length

$$l_B = \frac{e^2}{\epsilon kT} \tag{1}$$

The electrostatic interaction between two elementary charges $e$ separated by Bjerrum length $l_B$ in the solvent with dielectric constant $\epsilon$ is equal to the thermal energy $kT$ (where $k$ is the Boltzmann constant and $T$ is the absolute temperature). In a dilute salt-free solution, the charges on a chain interact with each other via an unscreened Coulomb potential. This electrostatic repulsion leads to chain stretching on length scales larger than the electrostatic blob size ($D_e$).[18−21] The conformation of a chain inside the electrostatic blob is almost unperturbed by electrostatic interactions, with the number of monomers in it being defined as $g_e \approx (D_e/a)^2$ in a $\theta$-solvent for the polymer backbone. The size $D_e$ of the electrostatic blob containing $g_e$ monomers can be found by comparing the electrostatic energy of a blob, $e^2 g_e^2 f^2/(\epsilon D_e)$, with the thermal energy $kT$. This leads to the electrostatic blob size being defined by the relation

$$D_e \approx a(uf^2)^{-1/3} \tag{2}$$

and the number of monomers in it,

$$g_e \approx (uf^2)^{-2/3} \tag{3}$$

where $u$ is the ratio of the Bjerrum length $l_B$ to the bond size $a$ ($u = l_B/a$). In the absence of salt, the polyelectrolyte configuration is that of a fully extended array of $N/g_e$ electrostatic blobs of contour length $L$:

$$L \approx \frac{N}{g_e} D_e \approx aN(uf^2)^{1/3} \tag{4}$$

The fully extended chain of electrostatic blobs is a fluctuating object. The typical mean-square fluctuations of the chain size in the longitudinal $\langle \delta L^2 \rangle$ and transverse $\langle R_\perp^2 \rangle$ directions are on the order of $a^2N$.

The electrostatic self-energy of the polyelectrolyte chain, $W_{elec}$, is proportional to the product of the thermal energy $kT$ and the number of electrostatic blobs, $N/g_e$, in the chain:

$$W_{elec} \approx kT\frac{N}{g_e} \approx kTN(uf^2)^{2/3} \tag{5}$$

A polyelectrolyte chain placed near a neutral adsorbing surface with an interaction contact energy of $-kT\epsilon_{vw}$ between the monomer and a surface is squashed by strong nonelectrostatic (van der Waals) attraction. The thickness of the adsorbed polyelectrolyte chain is on the order of the size of the adsorption blob ($\xi_{vw}$). The size of this blob can be found from the condition that its interaction with the adsorbing surface is on the order of the thermal energy $kT$ or $\epsilon_{vw} g_{vw}^{1/2} \approx 1$ (energy per contact $-kT\epsilon_{vw}$, multiplied by the number of contacts $g_{vw}^{1/2}$ between the adsorbing surface and the Gaussian strand with $g_{vw}$ monomers). This leads to the following expressions for the adsorption blob size,

$$\xi_{vw} \approx \frac{a}{\epsilon_{vw}} \tag{6}$$

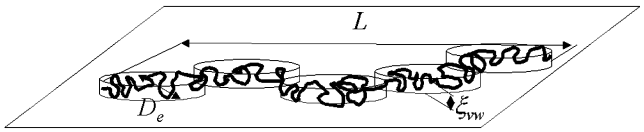


**Figure 1.** Schematic of a polyelectrolyte chain at an adsorbing surface. See text for definitions of the length scales.

and the number of monomers in it,

$$g_{vw} \approx \epsilon_{vw}^{-2} \tag{7}$$

The strong van der Waals attraction of a polyelectrolyte chain to a surface does not affect the longitudinal (in the plane of the adsorbing surface) size of the chain that is still controlled by electrostatic repulsion between charged monomers and is equal to $L$ (eq 4; see Figure 1). The adsorption energy of a polyelectrolyte chain due to short-range van der Waals interactions is proportional to the product of the thermal energy $kT$ and the number of adsorption blobs ($N/g_{vw}$) in a chain:

$$W_{vw} \approx -kT\frac{N}{g_{vw}} \approx -kT\epsilon_{vw}^2 N \tag{8}$$

However, in most experimental situations, such as the adsorption of polyelectrolyte chains from water onto clay, onto polymer latex surfaces, or at the water−air interface, the dielectric constant of the solvent $\epsilon$ is not equal to that of the surface $\epsilon_1$. The presence of the polyelectrolyte chain near the surface with dielectric constant $\epsilon_1$ causes the polarization of both media. The result is the appearance of an image polyelectrolyte chain located at the symmetric positions, with respect to the adsorbing surface[22] with a local charge,

$$q' = q\left(\frac{\epsilon - \epsilon_1}{\epsilon + \epsilon_1}\right) \approx q \tag{9}$$

for the nonpolar dielectric media with $\epsilon_1 \ll \epsilon$. The interaction of the polyelectrolyte chain with its image chain results in an additional repulsion with energy $W_{imag}$, defined as

$$W_{imag} \approx kT\frac{l_B(fN)^2}{L}\ln\left(\frac{L}{\xi_{vw}}\right) \approx kT\frac{N}{g_e} \approx W_{elec} \tag{10}$$

The repulsion of a polyelectrolyte chain from its image can be safely neglected if it is much smaller than the adsorption energy due to short-range interactions, $W_{vw}$. This condition is valid as long as the number of monomers in the electrostatic blob ($g_e$) is larger than the number of monomers in the adsorption blob ($g_{vw}$) or the energy per contact $\epsilon_{vw}$ satisfies the following inequality:

$$\epsilon_{vw} > (uf^2)^{1/3} \tag{11}$$

Below, we will assume that this inequality is always fulfilled, and we will ignore the effect of electrostatic interactions of the polyelectrolyte with its image chain.

## 3. Short-Range Attraction of Polyelectrolyte Chains to Adsorbing Charge Surfaces

**3.1. Dilute Two-Dimensional Adsorbed Layer (Regime I).** Consider the adsorption of polyelectrolyte chains at a charged surface with a surface charge density $e\sigma$ from a dilute polyelectrolyte solution with the Debye radius $r_D$ ($r_D^{-2} = 8\pi l_B \rho_s$, where $\rho_s$ is the salt concentration). Figure 2 summarizes our

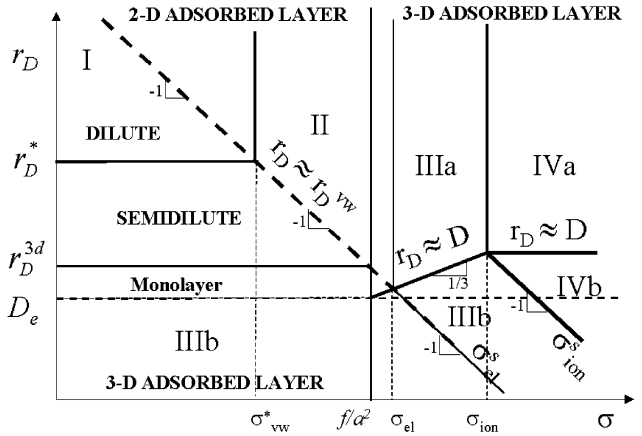


**Figure 2.** Adsorption diagram of polyelectrolyte chains at oppositely charged surfaces as a function of the surface charge number density $\sigma$ and the Debye radius $r_D$. (Logarithmic scales.)

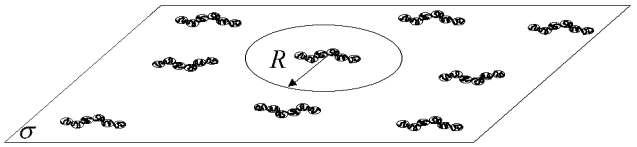


**Figure 3.** Schematic of the dilute two-dimensional adsorbed layer (regime I).

results in the form of the adsorption diagram in the surface charge number ($\sigma$)−Debye radius ($r_D$) plane. Following the results of our previous publications,[5,6,8] we will utilize a cell model to describe the adsorption layer. In this approach, each polyelectrolyte chain is assumed to be localized in the center of the cell of size $R$, because of the strong electrostatic repulsion between chains. The total electrostatic energy of an adsorbed polyelectrolyte chain includes the electrostatic attraction of the chain to the charged surface with a surface charge density $e\sigma$ (see Figure 3),

$$\frac{W_{att}}{kT} \approx -l_B f N \sigma \int_0^\infty \exp\left(-\frac{r}{r_D}\right) dr \approx -l_B f N \sigma r_D \qquad (12)$$

and repulsion from other adsorbed polyelectrolytes distributed with an effective surface charge density $efN/R^2$, starting at a distance $R$ from a given polyion:

$$\frac{W_{rep}}{kT} \approx \frac{l_B (fN)^2}{R^2} \int_R^\infty \exp\left(-\frac{r}{r_D}\right) dr \approx \frac{l_B (fN)^2 r_D}{R^2} \exp\left(-\frac{R}{r_D}\right) \qquad (13)$$

The total electrostatic energy of the adsorbed layer with the surface area $S$ is the sum of the contributions from all chains:

$$\frac{W_{Coul}}{kT} \approx S l_B r_D f N \left[\frac{1}{2}\left(\frac{fN}{R^4}\right) \exp\left(-\frac{R}{r_D}\right) - \frac{\sigma}{R^2}\right] \qquad (14)$$

The factor $^1/_2$ in front of the first term is added to avoid double-counting the repulsive interactions between the chains. (Note that, in the case of adsorption at a surface with low dielectric constant, each polyelectrolyte chain also interacts with image chains, as well as with the images of surface charges.)

The total free energy of the adsorbed layer in a dilute regime is the sum of the contributions from all chains due to electrostatic and short-range van der Waals interactions ($W_{vw}S/R^2$):

$$\frac{F}{kT} \approx S l_B r_D f N \left[\frac{1}{2}\left(\frac{fN}{R^4}\right) \exp\left(-\frac{R}{r_D}\right) - \frac{\sigma}{R^2}\right] - S\epsilon_{vw}^2 \left(\frac{N}{R^2}\right) \qquad (15)$$

The dependence of the cell size $R$ on the salt concentration is derived by minimizing the total free energy, with respect to $R$. The equilibrium cell size is the solution of the following equation:

$$\frac{fN}{R^2} \exp\left(-\frac{R}{r_D}\right)\left[1 + \frac{1}{4}\frac{R}{r_D}\right] \approx \sigma + \frac{\epsilon_{vw}^2}{l_B r_D f} \qquad (16)$$

It follows from the last equation that the cell size can either be obtained by balancing the electrostatic repulsion between chains with their attraction to the oppositely charged surface (the first term in the right-hand side of eq 16) or with their nonelectrostatic attraction to the adsorbing surface (the second term on the right-hand side of eq 16). The crossover between two stabilizing mechanisms takes place across the line (see Figure 2)

$$r_D^{vw} \approx \frac{\epsilon_{vw}^2}{l_B \sigma f} \qquad (17)$$

At low salt concentrations ($r_D > r_D^{vw}$), the cell size $R$ has a very weak dependence on the Debye screening length $r_D$. Thus, on the scaling level, we can assume that, at low salt concentrations, the size of the cell is

$$R \approx \sqrt{\frac{fN}{\sigma}} \qquad (\text{for } r_D > r_D^{vw}) \qquad (18)$$

The size of the cell is inversely proportional to the square root of the surface charge number density $\sigma$. At low salt concentrations, we can expand the left-hand side of eq 16 in the power series of $R/r_D$. After this expansion, eq 16 is reduced to

$$\frac{fN}{R^2}\left[1 - \frac{3}{4}\frac{R}{r_D}\right] \approx \sigma + \frac{\epsilon_{vw}^2}{l_B r_D f} \qquad (19)$$

Within this approximation, the overcharging of the charged surface by adsorbed polyelectrolyte chains is

$$\delta\sigma \approx \frac{fN}{R^2} - \sigma \approx \frac{3}{4}\frac{fN}{R r_D} + \frac{\epsilon_{vw}^2}{l_B r_D f} \approx \frac{\epsilon_{vw}^2}{l_B r_D f} \qquad (\text{for } r_D > r_D^{vw}) \qquad (20)$$

The surface overcharging, $\delta\sigma$, is independent of the bare surface charge density ($\sigma$) and increases with increasing strength of the van der Waals interactions and salt concentration. The surface overcharging $\delta\sigma$ becomes on the order of the bare surface charge density at the value of the Debye screening length $r_D \approx r_D^{vw}$.

When the Debye radius $r_D$ becomes smaller than $r_D^{vw}$, the electrostatic repulsion between adsorbed polyelectrolyte chains is balanced by their van der Waals attraction to the adsorbing surface. The cell size $R$ that minimizes the total free energy (see eq 15) is

$$R \approx \sqrt{r_D l_B N}\left(\frac{f}{\epsilon_{vw}}\right) \qquad (\text{for } r_D < r_D^{vw}) \qquad (21)$$

The cell size $R$ is proportional to the square root of the Debye radius $r_D$. The effective surface charge density in this high-salt

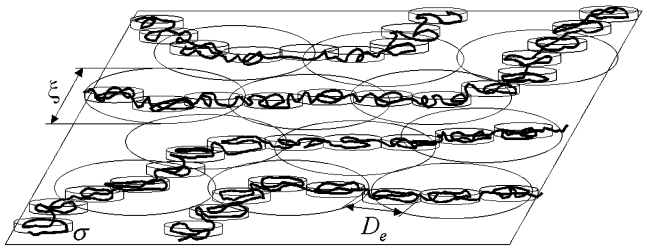


**Figure 4.** Schematic of the semidilute two-dimensional adsorbed layer (regime II).

concentration regime is

$$\delta\sigma \approx \frac{fN}{R^2} - \sigma \approx \frac{\epsilon_{vw}^2}{l_B r_D f} \qquad (\text{for } r_D < r_D^{vw}) \tag{22}$$

which has the same functional form as eq 20 and can be much larger than the bare surface charge number density $\sigma$.

As the surface charge number density $\sigma$ increases in the regime of low salt concentrations ($r_D > r_D^{vw}$), the cell size $R$ decreases and reaches the size of a polyelectrolyte chain ($L \approx aN(uf^2)^{1/3}$) at the surface charge number density.

$$\sigma_{vw}^* \approx \frac{1}{a^2 u^{2/3} f^{1/3} N} \qquad (\text{for } r_D > r_D^{vw}) \tag{23}$$

As the salt concentration increases in the regime of high salt concentrations ($r_D < r_D^{vw}$), the cell size $R$ decreases and reaches the size $L \approx aN(uf^2)^{1/3}$ at the value of the Debye radius that is given by

$$r_D^* \approx aN\frac{\epsilon_{vw}^2}{u^{1/3} f^{2/3}} \qquad (\text{for } r_D < r_D^{vw}) \tag{24}$$

These values of the surface charge number density $\sigma_{vw}^*$ and the Debye radius $r_D^*$ define the boundary between two-dimensional dilute and semidilute regimes (regimes I and II, respectively) in Figure 2.

**3.2. Semidilute Two-Dimensional Adsorbed Layer (Regime II).** In regime II, adsorbed polyelectrolytes arrange themselves into a two-dimensional semidilute polyelectrolyte solution, with the distance between chains ($\xi$) and the chain thickness, which is on the order of the adsorption blob size ($\xi_{vw}$), controlled by the van der Waals attraction of the polymer backbone to the adsorbing surface (see Figure 4). The intrachain electrostatic repulsion leads to chain stretching along the adsorbing surface on length scales larger than the electrostatic blob size $D_e$ (see Figure 4). At the length scales smaller than $\xi$, the polyelectrolyte configuration is that of a fully extended array of $g_\xi/g_e$ electrostatic blobs of contour length $\xi$:

$$\xi \approx \frac{g_\xi}{g_e} D_e \approx a g_\xi (uf^2)^{1/3} \tag{25}$$

To calculate the total free energy of the adsorbed layer, we once again divide the electrostatic contribution to the total free energy into the repulsive and attractive portions and add to it the contribution from the short-range van der Waals interactions. With these modifications, the free energy of the adsorbed layer is given as[8]

$$\frac{F}{kT} \approx S l_B r_D f g_\xi \left[\frac{f g_\xi}{2\xi^4} \exp\left(-\frac{\xi}{r_D}\right) - \frac{\sigma}{\xi^2}\right] - S\epsilon_{vw}^2 \left(\frac{g_\xi}{\xi^2}\right) \tag{26}$$

Minimizing this free energy $F$, with respect to the cell size $\xi$, and taking into account that $g_\xi \approx \xi/(u^{1/3} f^{2/3} a)$, one obtains the equation relating the cell size $\xi$ with the Debye radius $r_D$, the surface charge number density $\sigma$, and the adsorption energy $\epsilon_{vw}$:

$$\frac{f^{1/3}}{u^{1/3}\xi a}\left(1 + \frac{\xi}{2r_D}\right) \exp\left(-\frac{\xi}{r_D}\right) \approx \sigma + \frac{\epsilon_{vw}^2}{l_B r_D f} \tag{27}$$

At low salt concentrations ($r_D > r_D^{vw}$), the cell size (the correlation length of the two-dimensional semidilute solution),

$$\xi \approx \frac{f^{1/3}}{u^{1/3} a \sigma} \qquad (\text{for } r_D > r_D^{vw}) \tag{28}$$

is inversely proportional to the surface charge number density $\sigma$. The surface overcharging ($\delta\sigma$) in this regime,

$$\delta\sigma \approx \frac{\epsilon_{vw}^2}{l_B r_D f} \qquad (\text{for } r_D > r_D^{vw}) \tag{29}$$

is inversely proportional to the Debye radius $r_D$, is independent of the bare surface charge number density $\sigma$, and is similar to eqs 20 and 22.

At higher salt concentrations ($r_D < r_D^{vw}$), the solution of eq 27 is

$$\xi \approx r_D \frac{u^{2/3} f^{4/3}}{\epsilon_{vw}^2} \qquad (\text{for } r_D < r_D^{vw}) \tag{30}$$

Here, the distance between chains ($\xi$) scales linearly with the Debye screening length $r_D$. Thus, the distance between chains decreases as salt is added to the solution. The surface overcharging by adsorbed polyelectrolytes in the interval of salt concentrations ($r_D^{3d} < r_D < r_D^{vw}$) increases as the salt concentration increases.

$$\delta\sigma \approx \frac{f g_\xi}{\xi^2} - \sigma \approx \frac{\epsilon_{vw}^2}{l_B r_D f} \tag{31}$$

The two-dimensional electrostatic blobs start to overlap at the salt concentrations for which the cell size $\xi$ is on the order of the electrostatic blob size $D_e$. This occurs for the following value of the Debye radius $r_D$,

$$r_D^{3d} \approx D_e \frac{g_e}{g_{vw}} \approx a\frac{\epsilon_{vw}^2}{uf^2} \qquad (\text{for } r_D < r_D^{vw}) \tag{32}$$

and the surface charge number density,

$$\sigma_e \approx \frac{f}{a^2} \qquad (\text{for } r_D > r_D^{vw}) \tag{33}$$

(see Figure 2).

It is important to note that the structure of the adsorbed layer in regimes I and II is similar to that described previously in ref 8 for the case of the adsorption of hydrophobic polyelectrolytes at a hydrophobic surface with strong hydrophobic interactions between the polymer backbone and the adsorbing surface.

**3.3. Three-Dimensional Adsorbed Layer (Regimes III and IV).** *3.3.1. Low-Salt Regime IIIa.* At higher surface charge number densities ($\sigma > \sigma_e$), the polyelectrolyte chains form a concentrated polymer layer near the charged surface. In this case, the strong van der Waals attraction of the polymer backbone to the adsorbing surface controls the layer structure

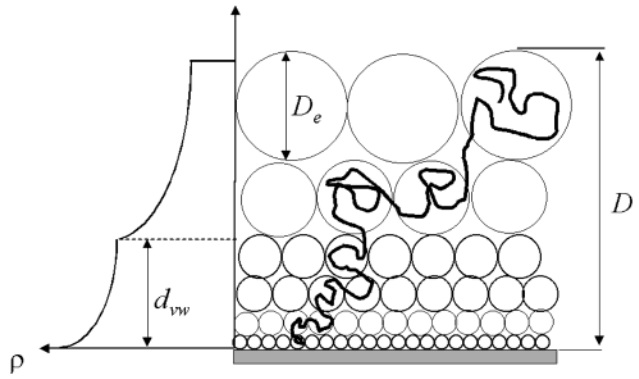


**Figure 5.** Polymer density profile in regime IIIa.

near the adsorbing surface (see Figure 5). In the vicinity of the charged surface, the polyelectrolytes form a self-similar polymer density profile that is given by the following expression:

$$\rho(z) \simeq \frac{1}{a^2(\xi_{vw} + z)} \tag{34}$$

This self-similar polymer density profile, which is known as de Gennes' carpet, was obtained by balancing the chain conformational entropy term with three-body interaction term in the way similar to that discussed in the paper by de Gennes.[23] The carpet ends at a distance $d_{vw}$ from a charged surface, where the polymer density $\rho(z)$ is determined by the balance of the electrostatic attraction to the charged surface with three-body monomer−monomer repulsion. The density profile of the salt ions in the electrostatic potential $\psi(z)$ at distance $z$ from the surface satisfies the Boltzmann distribution,

$$\rho_{\pm}(z) = \rho_{salt} \exp(\mp\varphi(z)) \tag{35}$$

where $\varphi(z)$ is the reduced electrostatic potential, defined as $\varphi(z) = e\psi(z)/(kT)$. The Poisson−Boltzmann equation for the reduced electrostatic potential at length scales $z < d_{vw}$ is

$$\frac{d^2\varphi(z)}{dz^2} = 4\pi l_B(f\rho(z) + \rho_-(z) - \rho_+(z)) = \frac{\varphi(z)}{r_D^2} + \frac{4\pi u f}{a(\xi_{vw} + z)} \tag{36}$$

together with the boundary condition at the charged surface,

$$\frac{d\varphi(z)}{dz}\Big|_{z=d_{vw}} = -4\pi l_B \sigma \tag{37}$$

At low salt concentrations ($\varphi(z)/r_D^2 < l_B f\rho(z)$), the polymer excess within the layer of thickness $d_{vw}$ results in the screening of the surface charge by the amount $fa^{-2}\ln(d_{vw}\epsilon_{vw}/a)$, reducing the surface charge density to

$$\sigma_{eff} \approx \sigma - \frac{f}{a^2}\ln\left(\frac{d_{vw}\epsilon_{vw}}{a}\right) \tag{38}$$

At the length scales $z > d_{vw}$, the distribution of the polymer density can be described within the framework of the mean-field approximation, assuming that the electrostatic interactions of a polymer with reduced external electrostatic potential $\varphi(z)$, created by other chains and the charged surface, dominates over the electrostatic self-energy of the chains. Following the results of our previous publications,[5−8] the relation between the reduced electrostatic potential $\varphi(z)$ and local polymer density $\rho(z)$ can be derived by assuming that the adsorbed layer is built of Gaussian blobs of size $\xi(z) \approx a\sqrt{g(z)}$. These blobs are densely packed with a local polymer density of $\rho(z) \approx g(z)/\xi^3(z)$. These blobs are multivalent sections of polyions with the valence $fg(z)$. Each blob interacts with the reduced electrostatic potential $\varphi(z)$, with an energy on the order of the thermal energy $kT$.

$$fg(z)\varphi(z) \approx 1 \tag{39}$$

This leads to the following relation between the monomer concentration $\rho(z)$ and the electrostatic potential $\varphi(z)$ at a distance $z$ from the surface:

$$\rho(z) \approx \frac{g(z)}{\xi^3(z)} \approx a^{-3}g(z)^{1/2} \approx a^{-3}(f\varphi(z))^{1/2} \tag{40}$$

The Poisson equation, which describes the distribution of the reduced electrostatic potential within the adsorbed layer in the presence of salt ions, has the form

$$\frac{d^2\varphi(z)}{dz^2} \approx \frac{\varphi(z)}{r_D^2} + 4\pi\left(\frac{uf^{3/2}}{a^2}\right)(\varphi(z))^{1/2} \qquad (\text{for } z > d_{vw}) \tag{41}$$

together with the boundary condition at a distance $z = d_{vw}$ from the charged surface:

$$\frac{d\varphi(z)}{dz}\Big|_{z=d_{vw}} = -4\pi l_B \sigma_{eff} \tag{42}$$

The polymer density profile in the adsorbed layer is obtained by solving this second-order nonlinear differential equation for the electrostatic potential $\varphi(z)$ (see eq 41):

$$\rho(z) = a^{-3}\sqrt{f\varphi(z)} = \frac{16\pi}{3}\left(\frac{uf^2r_D^2}{a^5}\right)\sinh^2\left(\frac{D-z}{4r_D}\right) \text{ (for } z > d_{vw}) \tag{43}$$

where $D$ is the layer thickness. At low salt concentrations ($D \ll r_D$, regime IIIa), the polymer density profile $\rho(z)$ has a parabolic form.

The thickness of the adsorbed layer, $D$, can be found from the boundary condition (eq 42):

$$\frac{64\pi}{9}\left(\frac{uf^3r_D^3}{a^3}\right)\sinh^3\left(\frac{D-d_{vw}}{4r_D}\right)\cosh\left(\frac{D-d_{vw}}{4r_D}\right) = \sigma_{eff}a^2 \tag{44}$$

The self-consistent equation that determines the thickness of the inner layer is obtained by matching the polymer density profile (eqs 34 and 43) at $z = d_{vw}$. For low salt concentrations ($D \ll r_D$), this equation is

$$\frac{\sigma a^2}{f} \approx \left(\frac{g_e}{g_{vw}}\right)^{3/4} y^{-3/2} + \ln y \tag{45}$$

where we introduce the parameter $y = d_{vw}/\xi_{vw}$. This equation has two solutions for the surface charge number density:

$$\sigma \gtrsim \sigma_{eq} \approx \frac{f}{a^2}\ln\left(\frac{D_e}{\xi_{vw}}\right) \tag{46}$$

From these two solutions, we must choose the one that has the lowest free energy. This solution is obtained by balancing the

left-hand side with the first term in the right-hand-side of eq 45:

$$d_{vw} \approx D_e\left(\frac{\sigma_e}{\sigma_{eff}}\right)^{2/3} \approx D_e\left(\frac{\sigma_e}{\sigma}\right)^{2/3} \quad (47)$$

The thickness $d_{vw}$ of the inner layer decreases as the surface charge density increases. At a surface charge number density of $\sigma \approx \sigma_e$, the thickness of the inner layer ($d_{vw}$) is on the order of the electrostatic blob size ($D_e$). The total thickness of the adsorbed layer ($D$) is obtained by solving eq 44. In the limit of low salt concentrations ($D - d_{vw} \ll r_D$), we recover the result

$$D \approx d_{vw} + a^{5/3}u^{-1/3}f^{-1}\sigma_{eff}^{1/3} \approx D_e\left(\frac{\sigma}{\sigma_e}\right)^{1/3} \quad (48)$$

obtained previously in refs 5 and 6. The thickness $D$ of the adsorbed layer increases as the one-third power of the surface charge number density $\sigma$.

In the interval of the surface charge number densities $\sigma_e \lesssim \sigma \lesssim \sigma_{eq}$, there is only an internal layer with a polymer density profile given by eq 34. The thickness of this layer is determined by the electroneutrality condition, which leads to its exponential growth with the surface charge number density $\sigma$.

$$D \approx d_{vw} \approx \xi_{vw}\exp\left(\frac{\sigma a^2}{f}\right) \quad (\text{for } \sigma_e \lesssim \sigma \lesssim \sigma_{eq}) \quad (49)$$

As the surface charge density increases further ($\sigma \gg \sigma_{eq}$), the inner portion of the adsorbed layer, which is controlled by the van der Waals attraction to a charged surface, shrinks and disappears completely at a surface charge number density $\sigma$ on the order of

$$\sigma_{el} \approx \sigma_e\left(\frac{D_e}{\xi_{vw}}\right)^{3/2} \quad (50)$$

For higher surface charge number densities ($\sigma > \sigma_{el}$), only electrostatic interactions between the polyelectrolytes and the adsorbing surface determine the structure of the adsorbed layer. (The boundary between these regimes is shown as a thin solid vertical line in the adsorption diagram in Figure 2.)

At the length scales $d_{vw} < z < D$, the adsorbed layer can be viewed as being built of blobs with size $\xi(z)$ increasing with distance $z$ from the surface:

$$\xi(z) \approx \frac{a^3}{uf^2r_D^2}\sinh^{-2}\left(\frac{D-z}{4r_D}\right) \quad (51)$$

As the surface charge density increases, the size of the first blob at the charged surface ($\xi(0) \approx a^{-1/3}u^{-1/3}\sigma^{-2/3}$) decreases. At the surface charge number density,

$$\sigma_{ion} \approx \frac{f^{3/4}}{a^2u^{1/2}} \quad (52)$$

the size of this blob will be on the order of the distance between charged monomers ($a/\sqrt{f}$) or there will be one charged monomer per such blob. This is the maximum possible screening of the surface by polyelectrolytes. A further increase of the polymer density near the surface is unfavorable, because of the high cost of the short-range monomer−monomer repulsive interactions. For the higher surface charge densities ($\sigma > \sigma_{ion}$), surface counterions start to dominate the screening of the surface potential near the surface, and the system crosses over into regime IVa. The line $\sigma \approx \sigma_{ion}$ determines the crossover to regime IVa. However, the vertical line $\sigma \approx \sigma_{el}$ is located to the left of the $\sigma \approx \sigma_{ion}$ line only when the van der Waals interaction parameter is $\epsilon_{vw} < \sqrt{f}$.

The surface undercharging by adsorbed polyelectrolytes in regime IIIa is obtained by integration of the polymer density profile $\rho(z)$ through the layer thickness $D$:

$$\delta\sigma_D = f\int_{d_{vw}}^{D}\rho(z)\,dz - \sigma \approx -\frac{a^{10/3}\sigma^{5/3}}{u^{2/3}f^2r_D^2} \quad (\text{for } \sigma > \sigma_{el}) \quad (53)$$

The addition of salt decreases the amount of polymer that is adsorbed, because salt ions also participate in the screening of the surface charge.

As we have shown in our previous publications,[5,6,8] the mean-field description of the polyelectrolyte adsorbed layer, presented previously, is incorrect within a distance $D_e$ from the outer boundary of the adsorbed layer. At these distances, the fluctuations of the polymer density $a^{-3}(uf^2)^{1/3}$ become larger than the average polymer density that is given by eq 43. This layer can be considered to be a two-dimensional melt of electrostatic blobs of size $D_e$. The surface overcharging due to this strongly fluctuating outer layer of electrostatic blobs can be estimated by comparing the attraction of the blobs to the charge surface with electrostatic repulsion between them. The effective surface charge number density $\Delta\sigma$ to which the last layer of thickness $D_e$ is subjected is on the order of the threshold value, $\sigma_e \approx fa^{-2}$. The attraction energy of an electrostatic blob to the charged background with the surface charge density $\sigma_e$ is

$$W_{att} \approx -kTl_B\sigma_eD_efg_e \approx -kT \quad (54)$$

The repulsion of the blob from all other blobs in this layer with the effective surface charge number density $\delta\sigma_e$ is

$$W_{rep} \approx kTl_B\delta\sigma_efg_er_D \quad (55)$$

At equilibrium, the total energy per blob in the adsorbed layer ($W_{att} + W_{rep}$) is equal to the chemical potential of the electrostatic blob in the bulk ($kTg_eN^{-1}\ln(\rho/N) + kT \approx kT$). This leads to surface overcharging due to this last layer of electrostatic blobs, by the amount of

$$\delta\sigma_e \approx \sigma_e\frac{D_e}{r_D} \approx \frac{f^{1/3}}{u^{1/3}ar_D} \quad (56)$$

The total overcharging of the adsorbing surface by polyelectrolyte chains is given as

$$\delta\sigma \approx \delta\sigma_e + \delta\sigma_D \approx \sigma_e\frac{D_e}{r_D} - \sigma\frac{D^2}{r_D^2} \quad (57)$$

The overcharging is equal to zero both in solutions with no added salt ($r_D = \infty$) and for

$$r_D^0 \approx \frac{\sigma D^2}{\sigma_eD_e} \approx \frac{a^{13/3}\sigma^{5/3}}{u^{1/3}f^{7/3}} \approx D_e\left(\frac{\sigma}{\sigma_e}\right)^{5/3} \quad (58)$$

At very low salt concentrations ($r_D > r_D^0$), the surface is overcharged by the adsorbed three-dimensional layer. At higher salt concentrations ($r_D < r_D^0$), the net charge of the adsorbed polyelectrolyte chains becomes smaller than the bare surface charge $\sigma$. The surface undercharging by the adsorbed polyelectrolyte chains is on the order of the bare surface charge number

density $\sigma$ when the Debye screening length $r_D$ is comparable to the layer thickness $D$.

$$r_D^D \approx D \approx a^{5/3}u^{-1/3}f^{-1}\sigma^{1/3} \tag{59}$$

For higher salt concentrations, the system crosses over to regime IIIb.

*3.3.2. High-Salt Regime IIIb.* At high salt concentrations ($r_D < r_D^D$), the salt ions dominate the screening of the charged surface. In this case, the solution of the Poisson−Boltzmann equation (eq 36) for the reduced electrostatic potential in the inner layer ($z < d_{vw}$) is

$$\varphi(z) \approx 4\pi l_B r_D \sigma \exp\left(-\frac{z}{r_D}\right) \tag{60}$$

The electrostatic attraction of polyelectrolytes to a charged surface becomes on the order of the three-body monomer−monomer repulsive interactions at a distance $d_{vw}$ from a charged surface, where

$$a^6\rho^2(d_{vw}) \approx \frac{a^2}{d_{vw}^2} \approx f\varphi(d_{vw}) \tag{61}$$

By combining eqs 60 and 61, we obtain the self-consistent equation for the thickness of the inner layer $d_{vw}$ as a function of the surface charge number density $\sigma$ and the Debye radius $r_D$:

$$\frac{\sigma a^2}{f}\exp\left(-\frac{d_{vw}}{r_D}\right) \approx \frac{D_e^3}{r_D\, d_{vw}^2} \tag{62}$$

The solution of this equation for the thickness of the inner layer in the limit $d_{vw} \le r_D$ is

$$d_{vw} \approx \frac{D_e^{3/2}}{r_D^{1/2}}\left(\frac{\sigma_e}{\sigma}\right)^{1/2} \tag{63}$$

The thickness $d_{vw}$ of this layer decreases as the surface charge number density $\sigma$ increases and increases as more salt is added to the solution. It becomes comparable to the size of the adsorption blob $\xi_{vw}$ at the surface charge number density

$$\sigma_{el}^s \approx \sigma_e\left(\frac{D_e^3}{r_D\,\xi_{vw}^2}\right) \approx \frac{\epsilon_{vw}^2}{l_B f r_D} \tag{64}$$

It is important to note that this line defines a crossover between electrostatically dominated and short-range-attraction-dominated adsorption regimes in the case of two-dimensional semidilute and dilute regimes (regimes I and II, respectively) in the adsorption diagram shown in Figure 2. (This line is shown as a thin solid line that coincides with the thick dashed line in the adsorption diagram.) The electrostatic attraction of polyelectrolyte chains to a charged surface control the layer structure for $\sigma > \sigma_{el}^s$.

The polymer concentration near the charged surface, $\rho(0) \approx a^{-3}\sqrt{f\varphi(0)} \approx a^{-3}\sqrt{l_B f r_D \sigma}$, increases as the surface charge density $\sigma$ increases. It reaches the maximum possible value $a^{-3}\sqrt{f}$ at the surface charge number density given by

$$\sigma_{ion}^s \approx \frac{1}{u r_D a} \tag{65}$$

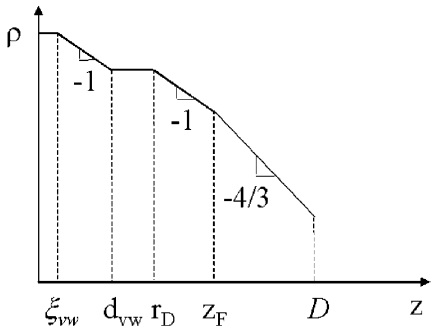


**Figure 6.** Polymer density profile in regime IIIb for the range of salt concentrations $r_D < D_e$. (Logarithmic scales.)

A further increase of the polymer concentration near the charged surface is unfavorable, because of the higher cost of the monomer−monomer repulsive interactions, and the system crosses over into regime IVb.

The $\sigma_{ion}^s$ and $\sigma_{el}^s$ lines are parallel to each other. Thus, the $\sigma_{el}^s$ line will be below the $\sigma_{ion}^s$ line only if the number of monomers in the adsorption blob ($1/\epsilon_{vw}^2$) is larger than the number of monomers between charges ($1/f$) or there is at least one charged monomer per adsorption blob ($\xi_{vw}$). If the opposite inequality holds, then the van der Waals interactions always control the structure of the adsorbed layer at the adsorbing surface. Here, we assume that $\epsilon_{vw} < \sqrt{f}$ and the structure of the adsorbed layer in a portion of regime III, as well as in the entire regime IV of the adsorption diagram (Figure 2), is similar to the structure discussed in our previous papers.[6,8]

The total thickness of the adsorbed layer is

$$D \approx \frac{D_e^{3/2}}{r_D^{1/2}}\left(\frac{\sigma_e}{\sigma_{eff}}\right)^{1/2} + r_D \ln\left(\frac{\sigma a^5}{u f^3 r_D^3}\right) \approx r_D \ln\left(\frac{\sigma a^5}{u f^3 r_D^3}\right) \quad (\text{for } D_e < r_D < r_D^D) \tag{66}$$

Thus, the thickness $D$ of the adsorbed layer is proportional to the Debye radius $r_D$.

The polymer surface excess ($\Gamma$) in the interval of the surface charge densities $\sigma < \sigma_{el}^s$ is the sum of three contributions that are due to the layer of thickness $d_{vw}$, the self-similar polyelectrolyte layer at length scales $d_{vw} < z < D$, and the thin layer of the size of the electrostatic blob $D_e$ at the edge of the self-similar layer:

$$\Gamma \approx \frac{1}{a^2}\ln\left(\frac{d_{vw}}{\xi_{vw}}\right) + \frac{\sigma}{f}\exp\left(-\frac{D}{2r_D}\right) + \frac{\sigma_e}{f}\left(\frac{D_e}{r_D}\right) \approx \left(\frac{\sigma u f r_D^3}{a^5}\right)^{1/2} \quad (\text{for } D_e < r_D < r_D^D) \tag{67}$$

The adsorbed layer begins to swell when the Debye radius $r_D$ becomes smaller than the electrostatic blob size $D_e$. In this range of salt concentrations, the intrachain electrostatic interactions can be treated as perturbations, and polyelectrolytes can be considered as neutral polymers with an excluded volume parameter $v \approx l_B r_D^2 f^2$. There are four different concentration regimes in the adsorption layer at high salt concentrations with $r_D < D_e$ (see Figure 6). Close to the charged surface at length scales of $z < d_{vw}$, the adsorbed polyelectrolyte forms the de Gennes' carpet with a polymer density that is inversely proportional to the distance from the charged surface $z$ ($\rho(z) \propto z^{-1}$; see eq 34). At the length scales $d_{vw} < z < r_D$, the polymer density profile in the adsorbed layer is determined by balancing the three-body monomer−monomer repulsive interactions ($a^6\rho^3(z)$)

with the electrostatic attraction to a charged surface ($\rho(z)f\varphi(z) \approx \rho(z)fl_B r_D\sigma \exp(-z/r_D)$). This leads to the almost-constant polymer density

$$\rho(z) \approx a^{-3}\sqrt{afl_B r_D\sigma}\exp\left(-\frac{z}{2r_D}\right) \approx a^{-3}\sqrt{fl_B r_D\sigma} \qquad (\text{for } r_D^{vw} < z < r_D) \quad (68)$$

At length scales of $z > r_D$, the electrostatic attraction to a charged surface is exponentially screened, and polyelectrolyte chains form the second layer of the de Gennes' carpet,[23] with the polymer density profile given by the following expression:

$$\rho(z) \approx a^{-3}\left(\frac{\sqrt{fl_B r_D^3\sigma}}{r_D + z}\right) \qquad (\text{for } r_D < z < z_F) \quad (69)$$

This layer is built by Gaussian blobs, the size of which ($\xi(z)$) grows linearly with the distance $z$ from a charged surface ($\rho(z) \approx g(z)/\xi(z)^3 \approx a^{-3}g^{-1/2}(z)$). The crossover to good solvent behavior occurs at a distance $z_F$ from the charged surface, where the two-body monomer−monomer repulsive interactions start to dominate the three-body interactions. At this distance $z_F$, the Fixman parameter ($v a^{-3}\sqrt{g(z_F)} \approx l_B r_D^2 f^2/(\rho(z)a^6)$) is on the order of unity. Using eq 69 for the density profile, one obtains the following expression for the distance $z_F$:

$$z_F \approx a^3\sqrt{\frac{\sigma}{f^3 l_B r_D}} \qquad \left(\text{for } D_e\left(\frac{\sigma_e}{\sigma}\right)^{1/3} < r_D < D_e\right) \quad (70)$$

The crossover distance $z_F$ increases as the salt concentration increases.

If the thickness $d_{vw}$ of the inner layer becomes on the order of the Debye screening length $r_D$, the regime of constant density (eq 68) disappears and the two de Gennes' carpets merge into a single one. In the interval of the salt concentrations such that

$$r_D < D_e\left(\frac{\sigma_e}{\sigma}\right)^{1/3} \quad (71)$$

the polymer density in the adsorbed layer is given by eq 34 in the entire interval $0 < z < z_F$, where $z_F$, in this case, is given as

$$z_F \approx \frac{a^4}{l_B r_D^2 f^2} \approx \frac{D_e^3}{r_D^2} \qquad \left(\text{for } r_D < D_e\left(\frac{\sigma_e}{\sigma}\right)^{1/3}\right) \quad (72)$$

At length scales $z > z_F$, there is also a self-similar de Gennes' carpet.[23] The density profile in this outer carpet is similar to that for neutral polymers with an excluded volume parameter $v \approx l_B r_D^2 f^2$ and decays as the distance $z$ from the surface increases (as $z^{-4/3}$; see Figure 6). The prefactor in the scaling expression for polymer density at length scales of $z_F < z$ can be obtained by matching the polymer density profiles at $z \approx z_F$. The thickness of the adsorbed layer is on the order of the chain size, with an excluded volume interaction parameter $v$:

$$D \approx v^{1/5}a^{2/5}N^{3/5} \approx a^{3/5}u^{1/5}f^{2/5}r_D^{2/5}N^{3/5} \qquad (\text{for } z_F < D) \quad (73)$$

For very high salt concentrations ($z_F > D$), the thickness of the adsorbed layer is that of a Gaussian chain ($a\sqrt{N}$). In this case, the region with $\rho(z) \approx z^{-4/3}$ disappears and the entire adsorbed layer has the same structure of a de Gennes' carpet (eq 34).

Regime IIIb also extends in the region of surface charge densities $\sigma < \sigma_e$ and $r_D < r_D^{3d}$. Here, the adsorbed polyelectrolytes first form a monolayer with a thickness on the order of adsorption blob ($\xi_{vw}$) for the values of the Debye radius $r_D$ larger than the electrostatic blob size $D_e$ ($D_e < r_D < r_D^{3d}$). This monolayer abruptly swells at $r_D \approx D_e$ when the layer thickness reaches the size of the neutral polymers with an excluded volume parameter $v \approx l_B r_D^2 f^2$ (see lower left portion of the adsorption diagram in Figure 2).

**3.4. Saturated Adsorbed Layer (Regime IV).** In this regime, the surface counterions control the screening of the surface charge near the surface. The polymer concentration near the surface is almost constant and is equal to

$$\rho(0) \approx a^{-3}f^{1/2} \quad (74)$$

whereas the concentration of the surface counterions is equal to

$$\rho_{ion}(z) \simeq \frac{\sigma^2 l_B}{(1 + \sigma l_B z)^2} \quad (75)$$

The concentration of surface counterions becomes comparable to the concentration of the charged monomers $f\rho(0)$ at the length scale

$$h \approx au^{-1/2}f^{-3/4} \quad (76)$$

At length scales of $z > h$, the structure of the adsorbed layer is similar to that in regime III. The polymer surface excess in this regime is given as

$$\Gamma \approx \frac{1}{u^{1/2}a^2f^{1/4}} + \frac{1}{u^{1/3}f^{2/3}ar_D} - \frac{a^{10/3}}{u^{3/2}f^{7/4}r_D^2} \qquad (\text{for low salt, } r_D > au^{-1/2}f^{-3/4})$$

$$\Gamma \approx \frac{f^{1/2}r_D}{a^3} \qquad (\text{for high salt, } r_D < au^{-1/2}f^{-3/4}) \quad (77)$$

If the interaction parameter $\epsilon_{vw}$ is larger than $\sqrt{f}$, the van der Waals attraction between the polymer backbone and the adsorbing surface changes the layer structure within the layer with thickness $a/\sqrt{f}$. Here, the polymer density decays hyperbolically, with a distance $z$ from the adsorbing surface (see eq 34). However, at length scales $z > a/\sqrt{f}$, the adsorbed layer has the same structure as that without van der Waals interactions.[6]

## 4. Adsorption of Polyelectrolyte Chains at Similarly Charged Surfaces

In the presence of strong van der Waals interactions, the polyelectrolyte chains can also be adsorbed at similarly charged surfaces. In this case, the adsorption takes place in the regions of the charge number density ($\sigma$)−Debye radius ($r_D$) plane where van der Waals attraction to the adsorbing surface dominates over the electrostatic repulsion between adsorbed polyelectrolyte chains and the similarly charged surface. The results for the adsorption diagram in this case can be easily derived again, using the results of section 3, and are summarized in Figure 7. In two-dimensional dilute and semidilute regimes (regimes I and II, respectively), the adsorption will take place below the $r_D \approx r_D^{vw}$ line (see eq 17), where van der Waals attractions are stronger than electrostatic repulsion from a charged surface. The

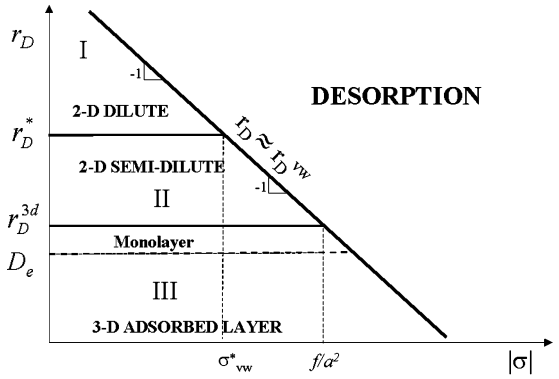


**Figure 7.** Adsorption diagram of polyelectrolyte chains at similarly charged surfaces as a function of the absolute value of the surface charge number density $|\sigma|$ and the Debye radius $r_D$. (Logarithmic scales.)

distance between chains in the dilute regime and the correlation length in the semidilute regime can be derived by substituting $-\sigma$ for $\sigma$ in eqs 15 and 27. The crossover between different regimes will be given by eqs 24 and 32.

In the interval of the salt concentrations such that $D_e < r_D < r_D^{3d}$, the adsorbed polyelectrolytes form a monolayer of adsorption blobs of size $\xi_{vw}$. The polyelectrolyte chains will be desorbed when the electrostatic repulsion of a blob from the charged surface, $kTl_B f\sigma r_D^2/\epsilon_{vw}^2$, is on the order of thermal energy $kT$. This occurs at the salt concentration for which the Debye radius is given as

$$r_D \approx r_D^{vw} \approx \frac{\epsilon_{vw}^2}{l_B f \sigma} \tag{78}$$

This is a continuation of the desorption line from the two-dimensional dilute and semidilute regimes.

The monolayer of adsorption blobs begins to swell when the Debye radius $r_D$ becomes smaller than the electrostatic blob size $D_e$. In this range of salt concentrations, the intrachain electrostatic interactions can be treated as perturbations and polyelectrolytes can be considered to be neutral polymers with an excluded volume parameter $v \approx l_B r_D^2 f^2$. The adsorption layer has two different concentration regimes. At the length scales $z < z_F$ (where $z_F = D_e^3/r_D^2$ ), the layer is built by Gaussian blobs, the size of which ($\xi(z)$) grows linearly with the distance $z$ from a charged surface, and polymer density is inversely proportional to the distance $z$ from a surface ($\rho(z) \approx z^{-1}$; see eq 34). At the length scales $z > z_F$, there is also a self-similar de Gennes' carpet.[23] In this carpet, the number of monomers in the blobs grows as the distance from a surface increases (as $z^{5/3}$). The density profile in this outer carpet decays as the distance $z$ from the surface increases (as $z^{-4/3}$). The thickness of this adsorbed layer is given by the size of the chain (see eq 73).

The polyelectrolyte chains are desorbed if the electrostatic repulsion between the charged surface and the section of the polyelectrolyte chain within a Debye radius $r_D$ is stronger than the van der Waals attraction between the surface and this section of the chain. The electrostatic repulsion between the section of adsorbed chain and the surface can be estimated as a Coulomb repulsion between the surface charge $\sigma r_D^2$ within a Debye radius $r_D$ and a polymeric charge $fr_D^2/a^2$ within a volume $r_D^3$ separated by a typical distance $r_D$. The Coulomb repulsion between those two charges is on the order of $kTl_B f\sigma r_D^3/a^2$. This electrostatic repulsion reaches the order of the van der Waals attraction ($-kT\epsilon_{vw}^2 r_D^2/a^2$) at a Debye radius of $r_D \approx r_D^{vw}$ (see eq 78).

## 5. Conclusion

We have presented a scaling analysis of polyelectrolyte adsorption that is due to strong short-range interactions. Our results are summarized in Figures 2 and 7, showing the adsorption diagrams in the plane of surface charge number density ($\sigma$)−Debye radius ($r_D$).

In the case of strong affinity between the polymer backbone and the adsorbing surface, the thickness of the two-dimensional dilute and semidilute adsorbed layers is determined by the short-range interactions and is inversely proportional to the adsorption energy $\epsilon_{vw}$. The polymer surface coverage ($\Gamma$) in these regimes is controlled either by the balance between electrostatic attraction to the oppositely charged surface and electrostatic repulsion between similarly charged chains at low salt concentrations (such that $r_D > r_D^{vw}$) or by the balance between the short-range attraction and electrostatic repulsion. For both dilute and semidilute two-dimensional adsorbed layers, the polymer surface coverage $\Gamma$ is inversely proportional to the Debye radius $r_D$ ($\Gamma \propto \rho_s^{1/2}$), thus, more polyelectrolytes can adsorb as salt concentration increases. This is not surprising, because the addition of salt leads to an exponential screening of the electrostatic repulsion between the polyelectrolyte chains.

A three-dimensional adsorbed layer is formed at surface charge densities $\sigma > f/a^2$. At low salt concentrations, the thickness of the three-dimensional adsorbed layer is initially proportional to $\sigma^{1/3}$ and then saturates at higher surface charge densities. The saturation of the layer thickness is due to an invasion of the adsorbed layer by the surface counterions. The cost to localize the counterions within the adsorbed layer is only on the order of the thermal energy $kT$ per counterion. It will cost substantially more to increase the polymer density near the adsorbing surface by the amount necessary to screen the surface charge, because of expensive three-body monomer−monomer repulsive interactions. Another interesting property of the three-dimensional adsorbed layer is nonmonotonic dependence of the polymer surface coverage on salt concentration. This nonmonotonic dependence is a manifestation of the two opposite tendencies. The addition of salt decreases the amount of adsorbed polymer inside the three-dimensional adsorbed layer because salt ions also participate in the screening of the surface charge. The increase in polymer surface coverage with increasing ionic strength is due to fluctuation−correlation effects at the edge of the adsorption layer. These two competing tendencies lead to the initial increase of the polymer surface excess at low salt concentrations (the fluctuation−correlation effects are dominant at low salt concentrations) and its decrease at moderate and higher salt concentrations, where the surface charge is mainly screened by salt ions. At very high salt concentrations, the electrostatic interactions can be treated as perturbations. In this regime, the structure of the adsorbed layer closely resembles that for neutral polymers with excluded volume interactions.

In the case of the adsorption of polyelectrolyte chains at similarly charged surfaces, the adsorption is possible only in the regimes where short-range attractive interactions between the polymer backbone and the adsorbing surface dominate the electrostatic repulsion between similarly charged chains and the charged surface. The qualitative features of adsorption regimes shown in Figure 7 are similar to the corresponding regimes in the adsorption diagram for polyelectrolyte chains at oppositely charged surfaces (see Figure 2) below the $r_D \approx r_D^{vw}$ line.

Let us estimate the typical $\sigma$ values for the boundaries between different regimes in the adsorption diagram (see Figures 2 and 7). Consider polyelectrolyte chains that consist of $N \approx$

$10^2$ Kuhn segments with size $a \approx 4$ Å adsorbing from an aqueous solution with the Bjerrum length $l_B = 7$ Å. If the fraction of charged monomers is $f \approx 0.1$, the boundaries between regimes in the adsorption diagram are $\sigma^*_{vw} \approx 10^{-3}$ Å$^{-2}$, $\sigma_e \approx 6 \times 10^{-3}$ Å$^{-2}$, and $\sigma_{ion} \approx 10^{-2}$ Å$^{-2}$. Thus, for such short chains, it is experimentally possible to study the full adsorption diagram. However, it should be noted that, for longer chains with $N \approx 10^3-10^5$ monomers, the experimentally accessible surface charge number densities will correspond to concentrated adsorbed layers in the three-dimensional adsorption regimes.

Our theory does not cover all aspects of polyelectrolyte adsorption. We only briefly mentioned the effect of the difference in the dielectric constants of solvent and adsorbing substrate on polyelectrolyte adsorption. The difference in the dielectric constants of the adsorbing substrate and the solvent can lead to some quantitative corrections but will not change the qualitative picture of polyelectrolyte adsorption that has been described in the present paper. Another effect that was not considered here is the charge regulation in the adsorbed layer. Many synthetic polyelectrolytes contain weak acidic or basic groups ("annealed" polyelectrolytes). The net charge on such molecules is dependent on the pH (and the ionic strength) of the solution. When such polyelectrolytes are adsorbed, the local electrostatic potential near a charged surface shifts the ionization equilibrium in the polyelectrolyte chains, altering the polymer and surface charge densities.[24] In this case, the altered ionic equilibrium is the additional driving force for overcompensation of the surface charge. Charge adjustment in the adsorbed layer can also occur for strong polyelectrolytes above their counterion condensation threshold. In this case, the system can reduce its free energy by releasing condensed counterions when a polymer chain is adsorbed at a surface. We will address these issues in future publications.

**Acknowledgment.** The authors are grateful to the National Science Foundation for the financial support (ECS-0103307, CHE-9876674, and DMR-0102267) and to the donors of the Petroleum Research Fund, administered by the American Chemical Society, for the financial support (37018-AC7).

## References and Notes

(1) Kawaguchi, M.; Takahashi, A. *Adv. Colloid Interface Sci.* **1992**, *37*, 219.
(2) Fleer, G. J.; Cohen Stuart, M. A.; Scheutjens, J. M. H. M.; Gasgove, T.; Vincent, B. *Polymers at Interfaces*; Chapman and Hall: London, 1993.
(3) Lyklema, J. *Fundamentals of Interface and Colloid Science: Solid−Liquid Interfaces*; Academic Press: London, 1995.
(4) Bajpai, A. K. *Prog. Polym. Sci.* **1997**, *22*, 523.
(5) Dobrynin, A. V.; Deshkovskii, A.; Rubinstein, M. *Phys. Rev. Lett.* **2000**, *84*, 3101.
(6) Dobrynin, A. V.; Deshkovskii, A.; Rubinstein, M. *Macromolecules* **2001**, *34*, 3421.
(7) Dobrynin, A. V. *J. Chem. Phys.* **2001**, *114*, 8145.
(8) Dobrynin, A. V.; Rubinstein, M. *Macromolecules* **2002**, *35*, 2754.
(9) Rouzina, I.; Bloomfield, V. *J. Phys. Chem.* **1996**, *100*, 9977.
(10) Perel, V. I.; Shklovskii, B. I. *Physica A* **1999**, *274*, 446.
(11) Shklovskii, B. I. *Phys. Rev. Lett.* **1999**, *82*, 3268
(12) Netz, R. R.; Joanny, J.-F. *Macromolecules* **1999**, *32*, 9026.
(13) Nguyen, T. T.; Grosberg, A. Yu.; Shklovskii, B. I. *Phys. Rev. Lett.* **2000**, *85*, 1588; *J. Chem. Phys.* **2000**, *113*, 1110.
(14) Varoqui, R. *J. Phys. II* **1993**, *3*, 1097.
(15) Borukhov, I.; Andelman, D.; Orland, H. *Europhys. Lett.* **1995**, *32*, 499.
(16) Joanny, J.-F. *Eur. Phys. J. B* **1999**, *9*, 117.
(17) Joanny, J.-F.; Castelnovo, M.; Netz, R. *J. Phys. Condens. Matter* **2000**, *12*, A1.
(18) de Gennes, P.-G.; Pincus, P.; Velasco, R. M.; Brochard, F. *J. Phys. (Paris)* **1976**, *37*, 1461.
(19) de Gennes, P.-G. *Scaling Concepts in Polymer Physics*; Cornell University Press: Ithaca, NY, 1979.
(20) Khokhlov, A. R.; Khachaturian, K. A. *Polymer* **1982**, *23*, 1742.
(21) Dobrynin, A. V.; Colby, R. H.; Rubinstein, M. *Macromolecules* **1995**, *28*, 1859.
(22) Jackson, J. D. *Classical Electrodynamics*; Wiley: New York, 1975.
(23) de Gennes, P. G. *Macromolecules* **1981**, *14*, 1637.
(24) Zhulina, E. B.; Dobrynin, A. V.; Rubinstein, M. *J. Phys. Chem. B* **2001**, *105*, 8917.